



Curvature driven flow of a family of interacting curves with applications

Michal Beneš¹ | Miroslav Kolář^{1,2} | Daniel Ševčovič³

¹Department of Mathematics, Faculty of Nuclear Sciences and Physical Engineering, Czech Technical University in Prague, Trojanova 13, Prague, 12000, Czech Republic

²Department of Mathematics, School of Science and Technology, Meiji University, 1-1-1 Higashi-Mita, Tama-ku, Kawasaki-shi, Kanagawa 214-8571, Japan

³Department of Applied Mathematics and Statistics, Faculty of Mathematics Physics and Informatics, Comenius University in Bratislava, Bratislava, Slovakia

Correspondence

Daniel Ševčovič, Department of Applied Mathematics and Statistics, Faculty of Mathematics Physics and Informatics, Comenius University in Bratislava, Bratislava, Slovakia.
Email: sevcovic@fmph.uniba.sk

Communicated by: T. Hishida

Funding information

International Research Fellowship of Japan Society for Promotion of Science; Ministry of Education, Youth and Sports of the Czech Republic under the OP RDE grant “Centre for Advanced Applied Sciences”, group MATE, Grant/Award Number: CZ.02.1.01/0.0/0.0/16 019/0000778; Vedecká Grantová Agentúra MŠVVaŠ SR a SAV, Grant/Award Number: 1/0062/18

In this paper, we investigate a system of geometric evolution equations describing a curvature-driven motion of a family of planar curves with mutual interactions that can have local as well as nonlocal character, and the entire curve may influence evolution of other curves. We propose a direct Lagrangian approach for solving such a geometric flow of interacting curves. We prove local existence, uniqueness, and continuation of classical Hölder smooth solutions to the governing system of nonlinear parabolic equations. A numerical solution to the governing system has been constructed by means of the method of flowing finite volumes. We also discuss various applications of the motion of interacting curves arising in nonlocal geometric flows of curves as well as an interesting physical problem of motion of two interacting dislocation loops in the material science.

KEYWORDS

curvature driven flow, flowing finite volume method, Hölder smooth solutions, interacting curves, nonlocal flow

MSC CLASSIFICATION

Primary: 35K57; 35K65; 65N40; 65M08; Secondary: 53C80

1 | INTRODUCTION AND PROBLEM DESCRIPTION

In this paper, we investigate a system of geometric evolution equations describing a curvature driven motion of a family of plane curves with mutual interactions.

Let $\Gamma^k, k = 1, \dots, n$ be a family of plane curves evolved in their respective outer normal directions \mathbf{n}^k by the velocities

$$v^k = -a^k \kappa^k + \mathcal{F}^k(\mathbf{x}^k, \mathbf{t}^k, \Gamma^1, \dots, \Gamma^n), \quad (1)$$

where κ^k is a curvature of the curve of Γ^k , and $\mathbf{t}^k, k = 1, \dots, n$, are their unit tangent vectors. The diffusion coefficient $a^k = a^k(\mathbf{x}^k, \mathbf{t}^k) > 0$ is assumed to depend locally on the position vector \mathbf{x}^k and the tangent vector \mathbf{t}^k . The nonlocal

functional \mathcal{F}^k is assumed to depend locally on the position and tangent vectors $\mathbf{x}^k, \mathbf{t}^k$, and globally on the entire family of curves $\Gamma^k, k = 1, \dots, n$. As an example, one can consider evolution of two ($n = 2$) interacting curves, where

$$\mathcal{F}^1(\mathbf{x}^1, \Gamma^2) = \int_{\Gamma^2} f^1(\mathbf{x}^1, \mathbf{X}^2(s^2)) ds^2, \quad \mathcal{F}^2(\mathbf{x}^2, \Gamma^1) = \int_{\Gamma^1} f^2(\mathbf{X}^1(s^1), \mathbf{x}^2) ds^1.$$

The curve Γ^k is parametrized by the mapping \mathbf{X}^k ; ie, $\Gamma^k = \{\mathbf{X}^k(s^k), s^k \in [0, L(\Gamma^k)]\}$, where s^k is the arc-length parametrization of Γ^k , $\mathbf{x}^k \in \Gamma^k$, and f^k are smooth functions for $k = 1, 2$. It means that the force \mathcal{F}^1 depends locally on the position vector \mathbf{x}^1 of the curve Γ^1 and nonlocally on the entire curve Γ^2 , and vice versa for the source term \mathcal{F}^2 . As another example, one can consider a simple nonlocal geometric flow of two interacting curves with external source terms given by

$$\mathcal{F}^1(\mathbf{x}^1, \Gamma^2) = \frac{2\pi}{L(\Gamma^2)}, \quad \mathcal{F}^2(\mathbf{x}^2, \Gamma^1) = \frac{2\pi}{L(\Gamma^1)},$$

and $L(\Gamma^k) = \int_{\Gamma^k} ds^k$ is the length of the curve Γ^k .

We follow the so-called direct Lagrangian approach in which the geometric evolution problem (1) for closed or open curves is treated by means of the parametric description. The direct Lagrangian approach was applied for planar curve evolution by many authors, eg, Deckelnick,¹ Beneš et al.,^{2,3} Mikula and Ševčovič,^{4–6} and others. In a previous article,⁷ Pauš et al. compared the direct approach and other interface-capturing methods, such as the level-set method or the phase-field method. In the paper⁷ by Pauš et al., the approximate algorithmic approach for handling topological changes (like self-intersecting) was proposed and analyzed. Concerning some of the drawbacks of the direct method, a problem of tangential redistribution was analyzed in previous studies^{8,9} by Ševčovič and Yazaki. An application of the direct approach to the system of geometrical flows (1) results to a system of degenerate parabolic equations for particular parametrizations of individual curves belonging to the family $\{\Gamma^1, \Gamma^2, \dots, \Gamma^n\}$. The system of governing equations is solved numerically to provide an information about the behavior of solutions to (1). The numerical approximation scheme is based on the flowing finite volume method that was proposed by Mikula and Ševčovič in their previous article⁴ for curvature driven flows of planar curves.

Applications of the investigated motion law described by (1) can be found in material science, especially in the models of discrete dislocation dynamics (see previous studies^{3,10,11}) or in the models of phase transitions (see previous studies^{12–15}) or in the models of recrystallization, in particular (cf Halberg¹⁶).

The paper is organized as follows. In the next section, we recall principles of the direct Lagrangian approach for solving curvature-driven flows of a family of interacting plane curves. We derive a system of nonlocal partial differential equations for parametrizations of evolving curves. Local existence, uniqueness, and continuation of classical Hölder smooth solutions is shown in section 3. A numerical discretization scheme based on the flowing finite volume method is presented in section 4. Examples of evolution of interacting curves are presented in section 5. First, we present a simple flow of two interacting curves in which nonlocal functionals depend on the total length of other curve. Next, we present an important physical application of evolution of open curves describing motion of interacting dislocation curves arising in the material science.

2 | LAGRANGIAN DESCRIPTION OF A MOTION OF INTERACTING CURVES

In the direct parametric Lagrangian approach, evolution of a family $\{\Gamma_t \subset \mathbb{R}^2, t \geq 0\}$ of planar time-dependent curves is described by the position vector $\mathbf{X} = \mathbf{X}(u, t) = (X_1(u, t), X_2(u, t))^T \in \mathbb{R}^2$, where $u \in [0, 1]$ is a parameter from the interval $I = [0, 1]$. Then, the curve Γ_t is given by

$$\Gamma_t = \{\mathbf{X}(u, t) = (X_1(u, t), X_2(u, t))^T, \quad u \in [0, 1]\}.$$

If we are dealing with closed curves for which \mathbf{X} is 1-periodic in the u variable, we will identify the interval $[0, 1]$ with $\mathbb{R}/\mathbb{Z} \equiv S^1$. Furthermore, we assume the parametrization of a closed curve Γ is oriented anticlockwise, and the periodic boundary conditions at $u = 0$ and $u = 1$ are imposed; ie, $\mathbf{X}|_{u=0} = \mathbf{X}|_{u=1}$, and $\partial_u \mathbf{X}|_{u=0} = \partial_u \mathbf{X}|_{u=1}$. In the case of evolution of open curves, we prescribe Dirichlet boundary conditions at $u = 0, 1$. That is, $\mathbf{X}(0) = \mathbf{a}, \mathbf{X}(1) = \mathbf{b}$ where \mathbf{a}, \mathbf{b} are prescribed endpoints $\mathbf{a} \neq \mathbf{b}$.

Geometric quantities such as the unit tangential vector \mathbf{t} and the outer unit normal vector \mathbf{n} can be expressed in terms \mathbf{X} as follows:

$$\mathbf{t} = \partial_u \mathbf{X} / |\partial_u \mathbf{X}| \text{ and } \mathbf{n} = \mathbf{t}^\perp = \partial_u \mathbf{X}^\perp / |\partial_u \mathbf{X}|,$$

where $\mathbf{x}^\perp = (x_2, -x_1)^T$ denotes the vector that is perpendicular to $\mathbf{x} = (x_1, x_2)^T$. Notice that the choice of the normal vector in the outer direction is in accordance with the rule $\det(\mathbf{n}, \mathbf{t}) = 1$. Let us denote the arc-length parametrization by s . Then, $ds = |\partial_u \mathbf{X}(u, t)| du$. The Frénet formulas yield $\partial_s \mathbf{t} = -\kappa \mathbf{n}$ and $\partial_s \mathbf{n} = \kappa \mathbf{t}$, where the curvature κ is given by the inner product:

$$\kappa = -\frac{1}{|\partial_u \mathbf{X}|} \frac{\partial}{\partial u} \left(\frac{\partial_u \mathbf{X}}{|\partial_u \mathbf{X}|} \right) \cdot \mathbf{n}.$$

Here, $\mathbf{a} \cdot \mathbf{b}$ stands for the Euclidean inner product of vectors \mathbf{a} and \mathbf{b} in \mathbb{R}^2 .

Next, we derive a system of evolution equations for position vectors $\mathbf{X}^k(u, t)$ describing curves Γ^k , $k = 1, \dots, n$. The family of planar curves $\{\Gamma^1, \Gamma^2, \dots, \Gamma^n\}$ evolves according to the system of geometric equations (1) provided that the parametrization $\mathbf{X}^k(u, t)$ satisfies the following system of nonlinear parabolic equations:

$$\partial_t \mathbf{X}^k = a^k \frac{1}{|\partial_u \mathbf{X}^k|} \frac{\partial}{\partial u} \left(\frac{\partial_u \mathbf{X}^k}{|\partial_u \mathbf{X}^k|} \right) + \mathcal{F}^k \mathbf{n}^k + \alpha^k \mathbf{t}^k, \quad \mathbf{X}^k|_{t=0} = \mathbf{X}_{ini}^k, \quad (2)$$

for $k = 1, 2, \dots, n$. Here, α^k is the tangential component of the velocity of the curve Γ^k . It is well-known that any tangential component of the velocity of Γ^k does not change its geometric shape (see e.g., Epstein and Gage¹⁷), and therefore, it is not important from the analytic point of view. However, concerning a numerical solution of (2), a suitable choice of a tangential velocity functional α^k plays an important role in construction of a stable numerical computational scheme. Various nontrivial choices of α^k have been proposed in the literature. We refer the reader to papers by Mikula and Ševčovič,^{5,6} Beneš et al.,^{3,7,18} and references therein. A general framework yielding the so-called curvature adjusted tangential velocity has been proposed by Ševčovič and Yazaki in a previous article.⁸ This approach takes into account variations in the curvature as well as the necessity of uniform or asymptotically uniform redistribution of points along evolved curves.

3 | LOCAL EXISTENCE AND CONTINUATION OF CLASSICAL SOLUTIONS

In this section, we prove local existence, uniqueness, and continuation of classical Hölder smooth solutions to the system of governing PDEs (2). To this purpose, we employ the so-called tangential velocities α_{uni}^k preserving the relative local length proposed and analyzed by Hou et al.,¹⁹ Kimura,²⁰ and Mikula and Ševčovič.⁵ Suppose that the tangential velocity $\alpha_{uni}^k(\mathbf{X}^k)$ nonlocally depends on the parametrization \mathbf{X}^k of the curve Γ^k and it is given by

$$\partial_u \alpha_{uni}^k = (-\kappa^k v^k + \langle \kappa^k v^k \rangle_{\Gamma^k}) |\partial_u \mathbf{X}^k|, \quad \alpha_{uni}^k|_{u=0} = 0, \quad (3)$$

where $\langle \kappa v \rangle_{\Gamma} = \frac{1}{L(\Gamma)} \int_{\Gamma} \kappa v ds$ is the curve average of the quantity κv . It can be shown that, for such a tangential velocity, we have the following identity:

$$\frac{|\partial_u \mathbf{X}^k(u, t)|}{L(\Gamma_t^k)} = \frac{|\partial_u \mathbf{X}^k(u, 0)|}{L(\Gamma_0^k)}, \quad \text{for all } u \in I, t \geq 0, \quad (4)$$

(cf Mikula and Ševčovič⁵). It means that the relative local length $|\partial_u \mathbf{X}^k(u, t)| / L(\Gamma_t^k)$ is constant with respect to time $t \geq 0$. Note that

$$\alpha_{uni}^k|_{u=1} = \alpha_{uni}^k|_{u=0} + \int_0^1 \partial_u \alpha_{uni}^k du = \int_{\Gamma_t^k} \left(-\kappa^k v^k + \langle \kappa^k v^k \rangle_{\Gamma_t^k} \right) ds^k = 0.$$

It means that there is no tangential motion of the endpoints $\mathbf{X}^k(0, t)$ and $\mathbf{X}^k(1, t)$.

Now, using the tangential velocity α_{uni} and inserting the term $|\partial_u \mathbf{X}^k(u, t)|$ from (4) into (2), the governing system of PDEs for evolution of the family of interacting curves (2) can be rewritten as follows:

$$\begin{aligned} \partial_t \mathbf{X}^k &= \frac{a^k L(\Gamma_0^k)^2}{(g_0^k(u) L(\Gamma^k))^2} \left(\partial_u^2 \mathbf{X}^k - \frac{\partial_u g_0^k}{g_0^k} \partial_u \mathbf{X}^k \right) + \mathcal{F}^k \mathbf{n}^k + \alpha_{uni}^k \mathbf{t}^k \\ &= \tilde{a}^k(u, \mathbf{x}^k, \mathbf{t}^k, L(\Gamma^k)) \left(\partial_u^2 \mathbf{X}^k - \frac{\partial_u g_0^k}{g_0^k} \partial_u \mathbf{X}^k \right) + \mathcal{F}^k \mathbf{n}^k + \alpha_{uni}^k \mathbf{t}^k, \\ \mathbf{X}^k|_{t=0} &= \mathbf{X}_{ini}^k, \end{aligned} \quad (5)$$

where

$$\tilde{a}^k(u, \mathbf{x}^k, \mathbf{t}^k, L(\Gamma^k)) = \frac{a^k (\mathbf{x}^k, \mathbf{t}^k) L(\Gamma_0^k)^2}{(g_0^k(u) L(\Gamma^k))^2}, \quad g_0^k(u) = |\partial_u \mathbf{X}^k(u, 0)|, \quad L(\Gamma^k) = \int_0^1 |\partial_u \mathbf{X}^k(u, \cdot)| du.$$

In the case of evolution of closed curves, we identify the interval $I = [0, 1]$ with $\mathbb{R}/\mathbb{Z} \equiv S^1$, and we impose periodic boundary conditions, ie,

$$u \mapsto \mathbf{X}^k(u, t) \text{ is a 1-periodic function, } k = 1, \dots, n.$$

In the case of evolution of open curves, we prescribe Dirichlet boundary conditions at $u = 0, 1$, ie,

$$\mathbf{X}^k(0, t) = \mathbf{a}^k, \quad \mathbf{X}(1, t) = \mathbf{b}^k, \quad k = 1, \dots, n,$$

where $\mathbf{a}^k \neq \mathbf{b}^k$ are given endpoints of an evolving open curve Γ_t^k .

In order to introduce underlying function spaces, we first introduce the shift function \mathbf{C}^k and the shifted solution $\tilde{\mathbf{X}}^k$

$$\begin{aligned} \tilde{\mathbf{X}}^k &= \mathbf{X}^k - \mathbf{C}^k, \\ \text{where } \mathbf{C}^k &\equiv 0, && \text{for closed curves evolution,} \\ \mathbf{C}^k(u) &= \mathbf{a}^k + u(\mathbf{b}^k - \mathbf{a}^k), && \text{for open curves evolution.} \end{aligned} \tag{6}$$

In what follows, we will identify the entire curve Γ^k with its parametrization, $\Gamma^k = \{\mathbf{X}^k(u), u \in I\}$ where the shifted parametrization $\tilde{\mathbf{X}}^k = \mathbf{X}^k - \mathbf{C}^k$ belongs to the function space E_1^{bc} . Here, $bc \in \{Pbc, Dbc\}$ stands for either periodic (*Pbc*) or homogeneous Dirichlet (*Dbc*) boundary conditions depending on whether closed or open curves evolution is studied. Here,

$$\begin{aligned} E_l^{Pbc} &= \{\tilde{\mathbf{X}} \in c^{2l+1+\epsilon}(I, \mathbb{R}^2), \quad I = \mathbb{R}/\mathbb{Z} \equiv S^1, \tilde{\mathbf{X}} \text{ is 1-periodic}\}, \quad l = 0, 1/2, 1, \\ E_l^{Dbc} &= \{\tilde{\mathbf{X}} \in c^{2l+1+\epsilon}(I, \mathbb{R}^2), \quad I = [0, 1], \quad \tilde{\mathbf{X}}(0) = \tilde{\mathbf{X}}(1) = 0\}, \quad l = 1/2, 1, \\ E_0^{Dbc} &= c^{1+\epsilon}(I, \mathbb{R}^2). \end{aligned} \tag{7}$$

Here, $c^{2l+1+\epsilon}, l = 0, 1/2, 1, 0 < \epsilon < 1$ is the little Hölder space consisting of $2l + 1 + \epsilon$ Hölder continuous functions (cf. Angenent²¹).

We will assume $\mathcal{F}^k = \mathcal{F}^k(\mathbf{x}^k, \mathbf{t}^k, \Gamma^1, \dots, \Gamma^n), k = 1, \dots, n$, is a mapping from the space $\mathbb{R}^2 \times \mathbb{R}^2 \times \mathcal{E}_{1/2}^{bc}$ into \mathbb{R} where

$$\mathcal{E}_l^{bc} = \underbrace{E_l^{bc} \times \dots \times E_l^{bc}}_{n-\text{times}}, \quad l = 0, 1/2, 1, \quad bc \in \{Pbc, Dbc\}.$$

Henceforth, we will suppose that a^k and \mathcal{F}^k satisfy the following smoothness assumptions:

$$a^k \in C^3(\mathbb{R}^2 \times \mathbb{R}^2, \mathbb{R}), \quad \mathcal{F}^k \in C^3(\mathbb{R}^2 \times \mathbb{R}^2 \times \mathcal{E}_{1/2}^{bc}, \mathbb{R}), \quad k = 1, \dots, n. \tag{8}$$

The system of equations (2) can be rewritten as an abstract evolution equation:

$$\partial_t \Phi = \mathcal{H}(\Phi), \quad \Phi(0) = \Phi_{ini} \equiv (\tilde{\mathbf{X}}_{ini}^k)_{k=1}^n, \tag{9}$$

in the space \mathcal{E}_0 where $\Phi = (\tilde{\mathbf{X}}^k)_{k=1}^n$. The mapping $\mathcal{H} : \mathcal{E}_1 \rightarrow \mathcal{E}_0$ defined by the right-hand side of (2) is C^1 smooth in the open neighborhood \mathcal{O}_1 of the initial condition $\Phi_{ini} \in \mathcal{O}_1 \subset \mathcal{E}_1$, where

$$\mathcal{O}_l = \{\Phi \in \mathcal{E}_l^{bc}, |\partial_u \mathbf{X}^k| > 0, k = 1, \dots, n\}, \quad \mathbf{X}^k = \tilde{\mathbf{X}}^k + \mathbf{C}^k, \quad l = 0, 1/2, 1.$$

Clearly,

$$\mathcal{H}(\Phi) = \mathcal{H}_0(\Phi) + \mathcal{H}_1(\Phi),$$

where $\mathcal{H}_0(\Phi)$ is the principal part of $\mathcal{H}(\Phi)$, and $\mathcal{H}_1 = \mathcal{H} - \mathcal{H}_0$ contains lower order terms, ie,

$$\mathcal{H}_0^k(\Phi) = \tilde{a}^k(u, \mathbf{x}^k, \mathbf{t}^k, L(\Gamma^k)) \partial_u^2 \mathbf{X}^k, \quad \mathcal{H}_1^k(\Phi) = -\tilde{a}^k \frac{\partial_u g_0^k}{g_0^k} \partial_u \mathbf{X}^k + \mathcal{F}^k \frac{(\partial_u \mathbf{X}^k)^\perp}{|\partial_u \mathbf{X}^k|} + a_{uni}^k \frac{\partial_u \mathbf{X}^k}{|\partial_u \mathbf{X}^k|},$$

where $\mathcal{F}^k = \mathcal{F}^k(\mathbf{x}^k, \mathbf{t}^k, \Gamma^1, \dots, \Gamma^n), \mathbf{t}^k = \partial_u \mathbf{X}^k / |\partial_u \mathbf{X}^k|$.

Lemma 1. Let $\bar{\Phi} \in \mathcal{O}_1 \subset \mathcal{E}_1$. The mapping $\mathcal{H} : \mathcal{O}_1 \subset \mathcal{E}_1 \rightarrow \mathcal{E}_0$ is C^1 differentiable at $\bar{\Phi}$. The linearization of the principal part \mathcal{H}_0 at $\bar{\Phi}$ in the direction $\Phi \in \mathcal{E}_1$ has the form: $[\mathcal{H}'_0(\bar{\Phi})\Phi]^k = \mathcal{A}\tilde{\mathbf{X}}^k + \mathcal{B}_0\tilde{\mathbf{X}}^k, k = 1, \dots, n$, where

$$\begin{aligned} \mathcal{A}\mathbf{X} &= \tilde{a}(u, \mathbf{x}, \bar{\mathbf{t}}, L(\bar{\Gamma})) \partial_u^2 \mathbf{X}, \\ \mathcal{B}_0 \mathbf{X} &= \left((\tilde{a}'_{\mathbf{t}} \cdot \bar{\mathbf{n}}) \frac{(\partial_u \mathbf{X} \cdot \bar{\mathbf{n}})}{|\partial_u \mathbf{X}|} + \tilde{a}'_{L(\bar{\Gamma})} \int_0^1 (\partial_u \mathbf{X}(u) \cdot \mathbf{t}(\bar{\mathbf{X}}(u))) du \right) \partial_u^2 \bar{\mathbf{X}}, \end{aligned}$$

where $\tilde{a} = \tilde{a}^k, \bar{\mathbf{X}} = \tilde{\mathbf{X}}^k, \bar{\mathbf{n}} = \bar{\mathbf{n}}^k, \bar{\mathbf{t}} = \bar{\mathbf{t}}^k$.

Proof. Let $\bar{\mathbf{X}} = \bar{\mathbf{X}}^k \in \mathcal{O}_1$ be a parametrization of the k -th curve $\bar{\Gamma} = \bar{\Gamma}^k$ and $\mathbf{X} \in E_1$. Denote $g(\mathbf{X}) = |\partial_u \mathbf{X}|$ and $\mathbf{t}(\mathbf{X}) = \partial_u \mathbf{X} / |\partial_u \mathbf{X}|$. Then, linearizations of g and \mathbf{t} at $\bar{\mathbf{X}}$ in the direction \mathbf{X} have the form:

$$g'(\bar{\mathbf{X}})\mathbf{X} = \partial_u \mathbf{X} \cdot \bar{\mathbf{t}}, \quad \mathbf{t}'(\bar{\mathbf{X}})\mathbf{X} = \partial_u \mathbf{X} / \bar{g} - (\partial_u \mathbf{X} \cdot \bar{\mathbf{t}}) \partial_u \bar{\mathbf{X}} / \bar{g}^2 = \frac{1}{\bar{g}} (\partial_u \mathbf{X} \cdot \bar{\mathbf{n}}) \bar{\mathbf{n}}.$$

Moreover, the linearization of the total length functional $L(\Gamma) = \int_{\Gamma} ds = \int_0^1 |\partial_u \mathbf{X}(u)| du = \int_0^1 g(\mathbf{X})(u) du$ is given by

$$L'(\bar{\Gamma})\mathbf{X} = \int_0^1 (\partial_u \mathbf{X}(u) \cdot \mathbf{t}(\bar{\mathbf{X}}(u))) du$$

and the proof of lemma follows. \square

Remark 1. Let $\tilde{g}(\tilde{\mathbf{X}}) = g(\mathbf{X})$ where $\mathbf{X} = \tilde{\mathbf{X}} + \mathbf{C}$. Then, the mapping $\tilde{g} : \mathcal{O}_1 \rightarrow c^{1+\epsilon}$ is C^1 differentiable. Indeed, for any $\mathbf{a}, \mathbf{b} \in \mathbb{R}^2$, we have $|\mathbf{a} + \mathbf{b}| - |\mathbf{a}| = \int_0^1 \frac{d}{d\xi} |\mathbf{a} + \xi \mathbf{b}| d\xi = \int_0^1 \frac{(\mathbf{a} + \xi \mathbf{b}) \cdot \mathbf{b}}{|\mathbf{a} + \xi \mathbf{b}|} d\xi$. Hence,

$$\begin{aligned} g(\bar{\mathbf{X}} + \mathbf{X}) - g(\bar{\mathbf{X}}) - g'(\bar{\mathbf{X}})\mathbf{X} &= \int_0^1 \frac{(\partial_u \bar{\mathbf{X}} + \xi \partial_u \mathbf{X}) \cdot \partial_u \mathbf{X}}{|\partial_u \bar{\mathbf{X}} + \xi \partial_u \mathbf{X}|} - \frac{\partial_u \bar{\mathbf{X}} \cdot \partial_u \mathbf{X}}{|\partial_u \bar{\mathbf{X}}|} d\xi \\ &= \int_0^1 \frac{(\xi |\partial_u \bar{\mathbf{X}}| \partial_u \mathbf{X} + (|\partial_u \bar{\mathbf{X}}| - |\partial_u \bar{\mathbf{X}} + \xi \partial_u \mathbf{X}|) \partial_u \bar{\mathbf{X}}) \cdot \partial_u \mathbf{X}}{|\partial_u \bar{\mathbf{X}} + \xi \partial_u \mathbf{X}| |\partial_u \bar{\mathbf{X}}|} d\xi. \end{aligned}$$

The little Hölder space $E_l = E_l^{bc}$ is a Banach algebra, ie, there exists $C > 0$ such that $\|\phi\psi\|_{E_l} \leq C \|\phi\|_{E_l} \|\psi\|_{E_l}$ for any $\phi, \psi \in E_l$. For any $\xi \in [0, 1]$, the $c^{1+\epsilon}$ norm of the integrated function is uniformly bounded in terms of the square of the norm $\|\mathbf{X}\|_{c^{1+\epsilon}}$. Hence, there exists a constant $C_0 > 0$ such that $\|\tilde{g}(\tilde{\mathbf{X}} + \tilde{\mathbf{X}}) - \tilde{g}(\tilde{\mathbf{X}}) - \tilde{g}'(\tilde{\mathbf{X}})\tilde{\mathbf{X}}\|_{c^{1+\epsilon}} \leq C_0 \|\tilde{\mathbf{X}}\|_{E_{1/2}}^2$. Therefore, $\tilde{g} \in C^1(\mathcal{O}_{1/2}, c^{1+\epsilon})$. A similar argument enables us to conclude that $\tilde{\mathbf{X}} \mapsto \mathbf{t}(\mathbf{X})$ is C^1 smooth mapping from $\mathcal{O}_{1/2}$ to E_0 and $\tilde{\mathbf{X}} \mapsto L(\Gamma)$ is C^1 smooth as a mapping from $\mathcal{O}_{1/2}$ to \mathbb{R} . As a consequence, the mapping \mathcal{H} is C^1 smooth from $\mathcal{O}_1 \subset \mathcal{E}_1$ to \mathcal{E}_0 , and its linearization is given by Lemma 1.

Now, we can state the following results on local existence, uniqueness, and continuation of solution.

Theorem 1. Assume the parametrization $\Phi_{ini} \equiv (\tilde{\mathbf{X}}_{ini}^k)_{k=1}^n$, of initial curves Γ_{ini}^k , belongs to the Hölder space \mathcal{E}_1^{bc} , and $|\partial_u \mathbf{X}_{ini}^k(u)| > 0$ for all $u \in I$ and $k = 1, \dots, n$. Assume $a^k(\mathbf{x}^k, \mathbf{t}^k)$ and $\mathcal{F}^k = \mathcal{F}^k(\mathbf{x}^k, \mathbf{t}^k, \Gamma^1, \dots, \Gamma^n)$ satisfies the assumption $\sim(8)$.

Then, there exists $T > 0$ and the unique family of curves $\{\Gamma_t^k, t \in [0, T]\}$ parametrized by $\mathbf{X}^k(\cdot, t) = \tilde{\mathbf{X}}^k(\cdot, t) + \mathbf{C}^k(\cdot)$ and evolving in the normal direction by the velocity v^k given by (1) and such that their shifted parametrization Φ satisfies $\Phi = (\tilde{\mathbf{X}}^k)_{k=1}^n \in C([0, T], \mathcal{E}_1^{bc}) \cap C^1([0, T], \mathcal{E}_0^{bc})$. Here, $bc = Pbc$ in the case of evolution of closed curves and $bc = Dbc$ in the case of evolution of open curves.

If the maximal time of existence $T_{max} < \infty$ is finite then,

$$\limsup_{t \rightarrow T_{max}} \sup_{k, \Gamma_t^k} |\kappa^k(\cdot, t)| = \infty.$$

Proof. The proof follows from the abstract resulting on existence, uniqueness of continuation of solutions to (9) due to Angenent²¹ in the scale of Banach spaces $\mathcal{E}_l = \mathcal{E}_l^{bc}$, $l = 0, 1$. It is based on the linearization of the abstract evolution equation (9) at arbitrary $\bar{\Phi} \in \mathcal{O}_1 \subset \mathcal{E}_1$ and showing that the linear operator $\mathcal{H}'(\bar{\Phi})$ belongs to the so-called maximal regularity class $\mathcal{M}(\mathcal{E}_\infty, \mathcal{E}_l)$. To this end, let $\bar{\Phi} \in \mathcal{O}_1 \subset \mathcal{E}_1$ be such that $|\partial_u \bar{\mathbf{X}}^k(u)| > 0$ for all $u \in I$ and $k = 1, \dots, n$. Then, $\tilde{a}^k(u, \mathbf{x}^k, \mathbf{t}^k, L(\bar{\Gamma}^k)) \in c^{1+\epsilon}(I, \mathbb{R})$ and $\tilde{a}^k > 0$. It follows from Angenent²¹ that the second order differential operator $-\mathcal{A}$ generates an analytic semigroup $\{e^{-\mathcal{A}t}, t \geq 0\}$ of operators in the Banach space \mathcal{E}_0 with the domain \mathcal{E}_∞ . Moreover, \mathcal{A} belongs to the so-called maximal regularity class $\mathcal{M}(\mathcal{E}_\infty, \mathcal{E}_l)$ consisting of all generators of analytic semigroups \mathcal{A} such that the initial value problem for the semilinear evolution equation: $\partial_t \phi - \mathcal{A} \phi = f(t), \phi(0) = \phi_0, t \in [0, T]$, has the unique solution $\phi \in C([0, T], \mathcal{E}_1) \cap C^1([0, T], \mathcal{E}_0)$ for any right-hand side $f \in C([0, T], \mathcal{E}_0)$ and an initial condition $\phi_0 \in \mathcal{E}_1$ and such that the inverse operator $(\partial_t - \mathcal{A})^{-1} : C([0, T], \mathcal{E}_0) \times \mathcal{E}_1 \mapsto C([0, T], \mathcal{E}_1) \cap C^1([0, T], \mathcal{E}_0)$ mapping the right-hand side f and the initial condition ϕ_0 to the solution ϕ is bounded (cf Angenent^{21,22}).

The operator \mathcal{B}_0 is a bounded linear operator from \mathcal{E}_∞ into \mathcal{E}_l . Furthermore, the curvature operator $\tilde{\kappa}(\tilde{\mathbf{X}}) = \kappa(\mathbf{X}) = \det(\partial_u \mathbf{X}, \partial_u^2 \mathbf{X}) / |\partial_u \mathbf{X}|^3$ is a C^1 mapping from the subset $O_{1/2} \subset E_{1/2}^{bc}$ of the Hölder space $E_{1/2} = c^{2+\epsilon}(I, \mathbb{R}^2)$ into $c^\epsilon(I, \mathbb{R})$, where $O_{1/2} = \{\tilde{\mathbf{X}} \in E_{1/2}, |\partial_u \mathbf{X}| > 0\}$ where $\mathbf{X} = \tilde{\mathbf{X}} + \mathbf{C}$. Taking into account smoothness assumptions made on coefficients a^k and \mathcal{F}^k , we conclude that the operator $\tilde{\mathbf{X}}^k \mapsto \partial_u a_{uni}^k(\mathbf{X}^k)$ is a C^1 smooth mapping from $E_{1/2} = c^{2+\epsilon}(I, \mathbb{R}^2)$

into $c^\varepsilon(I, \mathbb{R})$. As a consequence, $\alpha_{uni}^k \in C^1(E_{1/2}, c^{1+\varepsilon})$. Hence, the remaining lower order part operator $\mathcal{H}_1 \in C^1(\mathcal{E}_{\frac{1}{2}}, \mathcal{E}_0)$ and its linearization $\mathcal{B}_1 = \mathcal{H}'_1(\bar{\Phi})$ at $\bar{\Phi}$ is a bounded linear operator from $\mathcal{E}_{\frac{1}{2}}$ into \mathcal{E}_0 . In summary, $\mathcal{H} \in C^1(\mathcal{E}_1, \mathcal{E}_0)$ and $\mathcal{H}'(\bar{\Phi}) = \mathcal{A} + \mathcal{B}$ where $\mathcal{B} = \mathcal{B}_0 + \mathcal{B}_1$, $\mathcal{A} \in \mathcal{M}(\mathcal{E}_1, \mathcal{E}_0)$, $\mathcal{B} \in L(\mathcal{E}_{1/2}, \mathcal{E}_0)$. Taking into account the interpolation inequality between the Hölder spaces $c^{1+\varepsilon}$ and $c^{3+\varepsilon}$ spaces and the Young inequality $ab \leq \delta a^2 + b^2/(4\delta)$ valid for any $\delta > 0$, we conclude the following inequality:

$$\|\mathcal{B}\Phi\|_{\mathcal{E}_0} \leq C_1 \|\Phi\|_{\mathcal{E}_{\frac{1}{2}}} \leq C_0 \|\Phi\|_{\mathcal{E}_1}^{1/2} \|\Phi\|_{\mathcal{E}_0}^{1/2} \leq \delta \|\Phi\|_{\mathcal{E}_1} + K_\delta \|\Phi\|_{\mathcal{E}_0},$$

where $C_0, C_1, K_\delta = C_0^2/(4\delta) > 0$ are constants w.r. to Φ . Hence, the linear operator \mathcal{B} , now considered as a linear operator from \mathcal{E}_1 into \mathcal{E}_0 , has the so-called relative zero norm, ie, it satisfies the aforementioned inequality for any $\delta > 0$. With regard to Angenent²¹ (Lemma 2.5) (see also Lunardi²³), the maximal regularity class $\mathcal{M}(\mathcal{E}_1, \mathcal{E}_0)$ is closed with respect to perturbations by linear operators with the zero relative norm. Thus, $\mathcal{H}'(\bar{\Phi}) \in \mathcal{M}(\mathcal{E}_1, \mathcal{E}_0)$. Then, by applying the abstract theory on analytic semiflows due to Angenent²¹ (Theorem 2.7), we conclude local existence and uniqueness of solutions.

Finally, suppose to the contrary that $T_{max} < \infty$ and $\sup_{t < T_{max}, k, \Gamma_t^k} |\kappa^k(\cdot, t)| < \infty$. For any closed curve Γ , it holds: $2\pi = \int_{\Gamma} \kappa ds \leq L(\Gamma) \max_{\Gamma} |\kappa|$. In the case of an open curve with endpoints $\mathbf{a} \neq \mathbf{b}$, the length $L(\Gamma)$ is bounded from below by $\|\mathbf{a} - \mathbf{b}\| > 0$. In both cases, due to the definition and properties of the uniform tangential velocity α_{uni}^k (3)~the quantity $|\partial_u \mathbf{X}^k|$ is bounded from below in the lifespan $[0, T_{max}]$. In other words, the solution Φ does not attain a boundary of the open set \mathcal{O}_1 .

With regard to the results due to Mikula and Ševčovič⁴ the curvature $\kappa = \kappa^k$ is a solution to the parabolic equation

$$\partial_t \kappa = -\partial_s^2 v - \kappa^2 v + \kappa \partial_s \alpha_{uni} = \partial_s^2(a\kappa) - \partial_s^2 \mathcal{F} + \kappa \langle \kappa v \rangle_{\Gamma}, \quad \kappa(\cdot, 0) = \kappa_0(\cdot).$$

Because $\mathcal{F} = \mathcal{F}(\mathbf{x}, \mathbf{t}, \Gamma^1, \dots, \Gamma^n)$ and $\partial_s^2 \mathbf{t} = -\partial_s \kappa \mathbf{n} - \kappa^2 \mathbf{t}$, we have $-\partial_s^2 \mathcal{F} + \kappa \langle \kappa v \rangle_{\Gamma} = (\mathcal{F}'_{\mathbf{t}} \cdot \mathbf{n}) \partial_s \kappa + \mathcal{G}(\mathbf{x}, \mathbf{t}, \kappa, \Gamma^1, \dots, \Gamma^n)$, where \mathcal{G} is a smooth function that is bounded for κ belonging to a bounded set. Because $\kappa_0 \in c^{1+\varepsilon}$, the curvature κ is uniformly bounded in the norm of the space $c^{1+\varepsilon'}$ for $0 < t_0 \leq t < T_{max}$. Using compactness of the embedding of the space $c^{1+\varepsilon'}$ into $c^{1+\varepsilon}$ for $0 < \varepsilon < \varepsilon' < 1$, we conclude that the curvature κ can be continued up to the time $t = T_{max}$, and, consequently, there exists the limit $\lim_{t \rightarrow T_{max}} \mathbf{X}(\cdot, t) =: \bar{\mathbf{X}}$ in the space $E_1^{bc} \subseteq c^{3+\varepsilon}$. Starting from the initial condition $\bar{\mathbf{X}}$, we can continue the solution \mathbf{X} on some time interval $[T_{max}, T_{max} + T]$, beyond the maximal time of existence T_{max} , a contradiction. The proof of theorem follows. \square

4 | NUMERICAL APPROXIMATION SCHEME

Spatial discretization of (2) is based on the method of flowing finite volumes applied for solving general curvature driven flows. It was introduced and analyzed by Mikula and Ševčovič in their article.⁴ The basic idea of the method consists in consideration of the discrete nodes $\mathbf{x}_i = \mathbf{X}(u_i, t)$ for $i = 0, \dots, M$, $\mathbf{x}_0 = \mathbf{x}_M$, and $\mathbf{x}_1 = \mathbf{x}_{M+1}$. The dual discrete nodes $\mathbf{x}_{i \pm \frac{1}{2}} = \mathbf{X}(u_{i \pm \frac{1}{2}}, t)$ for $u_{i \pm \frac{1}{2}} = u_i \pm h/2$, $i = 1, \dots, M-1$, $h = 1/M$ are placed along the curve Γ as illustrated in Figure 1.

Then, parametric equations (2) are integrated over the dual finite volume $[u_{i-\frac{1}{2}}, u_{i+\frac{1}{2}}]$ surrounding the discrete node \mathbf{x}_i , $i = 1, \dots, M-1$. Integration results into the following expressions:

$$\int_{u_{i-\frac{1}{2}}}^{u_{i+\frac{1}{2}}} \partial_t \mathbf{X}^k |\partial_u \mathbf{X}^k| du = \int_{u_{i-\frac{1}{2}}}^{u_{i+\frac{1}{2}}} a^k \partial_u \left(\frac{\partial_u \mathbf{X}^k}{|\partial_u \mathbf{X}^k|} \right) + \mathcal{F}^k \partial_u (\mathbf{X}^k)^\perp + \alpha^k \partial_u \mathbf{X}^k du. \quad (10)$$

If we approximate the integrals in equation (10) by means of the finite volume method along the planar curve Γ^k , $k = 1, \dots, n$, we obtain:

$$\int_{u_{i-\frac{1}{2}}}^{u_{i+\frac{1}{2}}} \partial_t \mathbf{X}^k |\partial_u \mathbf{X}^k| du = \frac{d\mathbf{x}_i^k}{dt} \frac{d_{i+1}^k + d_i^k}{2},$$

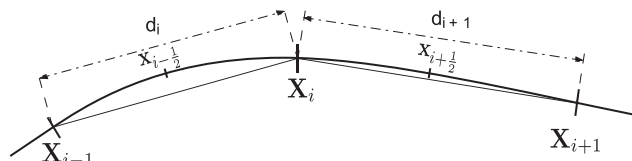


FIGURE 1 Discretization of a segment of a curve by flowing finite volumes

$$\begin{aligned} \int_{u_{i-\frac{1}{2}}}^{u_{i+\frac{1}{2}}} a^k \partial_u \left(\frac{\partial_u \mathbf{X}^k}{|\partial_u \mathbf{X}^k|} \right) du &= a_i^k \left(\frac{\mathbf{x}_{i+1}^k - \mathbf{x}_i^k}{d_{i+1}^k} - \frac{\mathbf{x}_i^k - \mathbf{x}_{i-1}^k}{d_i^k} \right), \\ \int_{u_{i-\frac{1}{2}}}^{u_{i+\frac{1}{2}}} \mathcal{F}^k \partial_u (\mathbf{X}^k)^\perp du &= \mathcal{F}_i^k \frac{(\mathbf{x}_{i+1}^k)^\perp - (\mathbf{x}_{i-1}^k)^\perp}{2}, \\ \int_{u_{i-\frac{1}{2}}}^{u_{i+\frac{1}{2}}} a^k \partial_u \mathbf{X}^k du &= a_i^k \frac{\mathbf{x}_{i+1}^k - \mathbf{x}_{i-1}^k}{2}, \quad d_i^k = |\mathbf{x}_i^k - \mathbf{x}_{i-1}^k|. \end{aligned}$$

Here, we assumed $\partial_t \mathbf{X}^k, \partial_u \mathbf{X}^k, a^k, \mathcal{F}^k, \alpha^k$ are constant over the dual finite volume $[u_{i-\frac{1}{2}}, u_{i+\frac{1}{2}}]$. Evaluation of the terms $a^k, \mathcal{F}^k, \alpha^k$ is based on the following approximation of the curvature, κ^k , tangent vector \mathbf{t}^k , and normal vector $\mathbf{n}^k = (\mathbf{t}^k)^\perp$:

$$\kappa_i^k = -\frac{2}{d_i^k + d_{i+1}^k} \left(\frac{\mathbf{x}_{i+1}^k - \mathbf{x}_i^k}{d_{i+1}^k} - \frac{\mathbf{x}_i^k - \mathbf{x}_{i-1}^k}{d_i^k} \right) \cdot \mathbf{n}_i^k, \quad \mathbf{t}_i^k = \frac{\mathbf{x}_{i+1}^k - \mathbf{x}_{i-1}^k}{d_{i+1}^k + d_i^k}. \quad (11)$$

The nonlocal functional \mathcal{F}^k is approximated by $\mathcal{F}_i^k = \mathcal{F}^k(\mathbf{x}_i^k, \mathbf{t}_i^k, \hat{\Gamma}^1, \dots, \hat{\Gamma}^n)$ where the curve Γ^l entering the definition of \mathcal{F}^k is approximated by the polygonal curve $\hat{\Gamma}^l$ with vertices $(\mathbf{x}_1^l, \dots, \mathbf{x}_M^l)$. Finally, for the approximation of the tangential velocity α_{uni}^k introduced as in (3) we apply a simple integration rule (using the boundary condition $\alpha_{uni}^k|_{u=0} = 0$), ie, $\alpha_i^k = \sum_{j=1}^i (-\kappa_j^k v_j^k + \langle \kappa^k v^k \rangle_{\Gamma^k}) d_j^k$ where $v_i^k = a_i^k \kappa_i^k + \mathcal{F}_i^k$ and $\langle \kappa^k v^k \rangle_{\Gamma^k} = (\sum_{j=1}^M \kappa_j^k v_j^k) / L^k$, and L^k is the length of the approximating polygonal curve $\hat{\Gamma}^k$, ie, $L^k = \sum_{j=1}^M d_j^k$.

In summary, the semidiscrete scheme for solving (2) can be rewritten as follows:

$$\begin{aligned} \frac{d\mathbf{x}_i^k}{dt} \frac{d_{i+1}^k + d_i^k}{2} &= a_i^k \left(\frac{\mathbf{x}_{i+1}^k - \mathbf{x}_i^k}{d_{i+1}^k} - \frac{\mathbf{x}_i^k - \mathbf{x}_{i-1}^k}{d_i^k} \right) \\ &\quad + \mathcal{F}_i^k \frac{(\mathbf{x}_{i+1}^k)^\perp - (\mathbf{x}_{i-1}^k)^\perp}{2} + a_i^k \frac{\mathbf{x}_{i+1}^k - \mathbf{x}_{i-1}^k}{2}, \end{aligned} \quad (12)$$

$$\mathbf{x}_i^k(0) = \mathbf{X}_{ini}^k(u_i), \quad \text{for } i = 1, \dots, M. \quad (13)$$

Systems (12)–(4) of ODEs are then solved numerically by means of the 4th-order explicit Runge-Kutta-Merson scheme with the automatic time stepping control with the tolerance parameter 10^{-6} (see previous studies¹⁸ or³). We chose the initial time-step as $4h^2$, where $h = 1/M$ is the spatial mesh size.

5 | APPLICATIONS IN NONLOCAL GEOMETRIC FLOWS AND DISLOCATION DYNAMICS

In this section, we present two model examples of geometric flows of two interacting curves. The first example presented in Section 5.1.1 is a generalization of the area preserving flow of a single curve introduced and investigated by Gage.²⁴ We will show that a formal generalization of the area preserving flow for two interacting curves lead to the total length shortening and total area enlarging flow. This example also serves as a motivation for the flow of two interacting dislocation loops with nonlocal interactions investigated in Section 5.2.

The purpose of the second example presented in Section 5.1.2 is to show that a nonlocal curvature driven flow of n interacting curves with nonlocal source terms may exhibit the same complicated dynamics as the flow generated by a system ordinary differential equations in \mathbb{R}^n including, in particular, chaotic behavior for $n \geq 3$.

5.1 | Geometric flows of interacting closed curves

5.1.1 | Length shortening and area enlarging nonlocal geometric flows

Recall that the flow of a single closed Jordan curve Γ evolved in the outer normal direction by the velocity:

$$v = -\kappa + \frac{2\pi}{L(\Gamma)}$$

is the area preserving and the total length shortening flow of planar curves. It was proposed and investigated by Gage.²⁴ These properties easily follow from the identities:

$$\frac{d}{dt}L(\Gamma_t) = \int_{\Gamma_t} v\kappa ds, \quad \frac{d}{dt}A(\Gamma_t) = \int_{\Gamma_t} vds, \quad \int_{\Gamma_t} \kappa ds = 2\pi, \quad (14)$$

where $L(\Gamma_t)$ and $A(\Gamma_t)$ are the total length and enclosed area of the evolved curve Γ_t , $t \geq 0$.

In this section, we present and analyze an example of two closed interacting planar curves with the nonlocal interaction source terms given by:

$$v^1 = -\kappa^1 + \frac{2\pi}{L(\Gamma^2)}, \quad v^2 = -\kappa^2 + \frac{2\pi}{L(\Gamma^1)}. \quad (15)$$

It means that the nonlocal source terms involve the total length of the other curve. In the following proposition, we present basic properties of such a flow of interacting curves.

Proposition 1. *Assume that $\{\Gamma_t^i, t \geq 0\}$, $i = 1, 2$ are two families of Jordan curves evolved in the outer normal direction by the normal velocities v^i given as in (15). Then, the sum and product of their total lengths of both curves is nonincreasing and the sum of the enclosed areas is nondecreasing, that is*

$$\frac{d}{dt}(L(\Gamma_t^1) + L(\Gamma_t^2)) \leq 0, \quad \frac{d}{dt}(L(\Gamma_t^1)L(\Gamma_t^2)) \leq 0, \quad \frac{d}{dt}(A(\Gamma_t^1) + A(\Gamma_t^2)) \geq 0, \quad \text{for all } t \geq 0.$$

Proof. We have

$$\begin{aligned} \frac{d}{dt}(L(\Gamma_t^1) + L(\Gamma_t^2)) &= \int_{\Gamma_t^1} v^1 \kappa^1 ds^1 + \int_{\Gamma_t^2} v^2 \kappa^2 ds^2 \\ &= - \int_{\Gamma_t^1} (\kappa^1)^2 ds^1 + \frac{4\pi^2}{L(\Gamma_t^2)} - \int_{\Gamma_t^2} (\kappa^2)^2 ds^2 + \frac{4\pi^2}{L(\Gamma_t^1)} \leq 0, \end{aligned}$$

due to the Cauchy-Schwartz inequality:

$$4\pi^2 = \left(\int_{\Gamma_t^i} \kappa^i ds^i \right)^2 \leq \int_{\Gamma_t^i} 1 ds^i \int_{\Gamma_t^i} (\kappa^i)^2 ds^i = L(\Gamma_t^i) \int_{\Gamma_t^i} (\kappa^i)^2 ds, \quad i = 1, 2. \quad (16)$$

Similarly, for the product of total lengths we obtain

$$\begin{aligned} \frac{d}{dt}(L(\Gamma_t^1)L(\Gamma_t^2)) &= -L(\Gamma_t^2) \int_{\Gamma_t^1} (\kappa^1)^2 ds^1 + 4\pi^2 - L(\Gamma_t^1) \int_{\Gamma_t^2} (\kappa^2)^2 ds^2 + 4\pi^2 \\ &\leq 4\pi^2 \left(2 - \frac{L(\Gamma_t^2)}{L(\Gamma_t^1)} - \frac{L(\Gamma_t^1)}{L(\Gamma_t^2)} \right) = -4\pi^2 \frac{(L(\Gamma_t^1) - L(\Gamma_t^2))^2}{L(\Gamma_t^1)L(\Gamma_t^2)} \leq 0 \end{aligned}$$

again due to the Cauchy-Schwartz inequality (16). Finally,

$$\begin{aligned} \frac{d}{dt}(A(\Gamma_t^1) + A(\Gamma_t^2)) &= \int_{\Gamma_t^1} v^1 ds^1 + \int_{\Gamma_t^2} v^2 ds^2 = -2\pi + \frac{2\pi L(\Gamma_t^1)}{L(\Gamma_t^2)} - 2\pi + \frac{2\pi L(\Gamma_t^2)}{L(\Gamma_t^1)} \\ &= 2\pi \left(-2 + \frac{L(\Gamma_t^2)}{L(\Gamma_t^1)} + \frac{L(\Gamma_t^1)}{L(\Gamma_t^2)} \right) = 2\pi \frac{(L(\Gamma_t^1) - L(\Gamma_t^2))^2}{L(\Gamma_t^1)L(\Gamma_t^2)} \geq 0, \end{aligned}$$

as claimed. \square

5.1.2 | Embedding of arbitrary finite dimensional dynamics into the flow of interacting curves

It is well known that systems of autonomous ordinary differential equations of the form:

$$\frac{dr}{dt} = f(r), \quad (17)$$

where $f = (f_1, \dots, f_n)^T \in C^1(\mathbb{R}^n, \mathbb{R}^n)$, may exhibit complicated dynamics, eg, existence of a stable periodic orbit in the phase space \mathbb{R}^2 or chaotic dynamics including the strange Lorentz attractor in \mathbb{R}^3 , etc.

If the family of interacting curves evolves according to geometric equations (1) where

$$v^k = -\kappa^k + \frac{2\pi}{L(\Gamma^k)} + f_k(L(\Gamma^1), \dots, L(\Gamma^n)), \quad k = 1, \dots, n, \quad (18)$$

then the dynamics of (17) is included in (18) in the sense that the evolving family of plane circles with radii r_k , have the same dynamical behavior as solutions to (17).

As an example of embedding of the finite dimensional ODE dynamics into the interacting curves evolution, we present a system of two interacting curves with prescribed Lotka-Volterra dynamics. In this system of evolving curves with interactions, the outer normal velocities have the following form:

$$v^1 = -\kappa^1 + \frac{2\pi}{L(\Gamma^1)} + L(\Gamma^1)(\alpha - \beta L(\Gamma^2)), \quad v^2 = -\kappa^2 + \frac{2\pi}{L(\Gamma^2)} + L(\Gamma^2)(\delta L(\Gamma^1) - \gamma). \quad (19)$$

Suppose that the evolving curves are circles with time dependent radii $r_i, i = 1, 2$. Because $-\kappa + \frac{2\pi}{L(\Gamma)} = 0$ for any circle Γ , we obtain the system of ordinary differential equations for r_i , ie,

$$\frac{d}{dt}r_1 = 2\pi r_1(\alpha - 2\pi\beta r_2), \quad \frac{d}{dt}r_2 = 2\pi r_2(2\pi\delta r_1 - \gamma), \quad (20)$$

which is the well known Lotka-Volterra system of ODEs describing the dynamics of the predator-prey system.

Periodically oscillating solutions of (19) for the initial 5-leaf shape and Ying-Yang shape curves is shown in Figure 2. Both curves attain circular shapes and their radii converge to the periodic orbit with parameters $\alpha = 1/(2\pi)$, $\beta = 2/(3\pi^2)$, $\gamma = 1/(2\pi)$, $\delta = 1/(4\pi^2)$.

5.2 | Dynamics of curves describing interaction of dislocation loops in different parallel slip planes

In this section, we present an important physical application of a geometric flow of two interacting curves (1) describing the motion of dislocation loops arising in the dislocation dynamics. It is known that real crystalline solids may contain imperfections in their crystal lattice. Some of those imperfections can be represented either as closed curves inside the crystal or as open curves ending on the crystal surface that evolve in time and are given slip planes.³ Dislocations were experimentally observed in 1950's (cf Hirsch et al.²⁵). Nowadays, the dynamics of dislocations is considered as one of key elements for better understanding of crystal plasticity. For more references on the dislocation dynamics theory, we refer the reader to, eg,^{26,27}. As a mathematical model, we can consider the motion of a pair of dislocation curves Γ^1 and Γ^2 moving against each other in parallel slip planes with the fixed distance $h_0 > 0$. The dislocations are driven by the uniform external stress, and they evolve inside the so-called persistent slip band channel.^{3,28,29} The channel represents natural boundary for their motion, and mutual force interactions between both dislocations are considered. A geometric flow of two interacting dislocation loops has the form of (1), ie,

$$\beta v^1 = -\gamma^1 \kappa_\Gamma^1 + \mathcal{F}^1, \quad \beta v^2 = -\gamma^2 \kappa_\Gamma^2 + \mathcal{F}^2,$$

where $\beta > 0$ is the drag coefficient, and $\gamma^k > 0$ is the line tension approximated as

$$\gamma^k = \frac{3}{4}Gb^2(1 - 2\nu + 3\nu\cos^2\xi^k),$$

where G , and ν are material parameters, and ξ^i is the angle between the x -axis and the tangent to dislocation $\Gamma^k, k = 1, 2$. The parameter b is the magnitude of the so-called Burgers vector $\mathbf{b} = (b, 0, 0)^T$ (cf Pauš et al.¹⁰ and Kolář et al.³⁰). The external source terms $\mathcal{F}^k, k = 1, 2$, have the following form:

$$\mathcal{F}^k = b(\tau_{app}^k + \tau_{wall}^k + \tau_{int}^k),$$

where $\tau_{app}^k + \tau_{wall}^k + \tau_{int}^k$ is the sum of resolved shear stresses considered in the model (cf previous studies^{3,7,30}). Here, τ_{app}^k is the external applied stress; τ_{wall}^k denotes the elastic field generated from the walls of the channel of the respective dislocation. It can be approximated by means of rational functions in the X_1^k variable of the parametrization \mathbf{X}^k as it was explained in previous studies,^{3,30} where appropriate formulas can be found. Finally, $\tau_{int}^k, k = 1, 2$ represent interaction stress fields from one dislocation loop to the another one. Because dislocations are represented as piece-wise linear curves, one needs to determine the stress tensor $\sigma_{ij}^{AB} = \sigma_{ij}^{AB}(\mathbf{x}), i, j = 1, 2, 3$, at $\mathbf{x} \in \mathbb{R}^3$ from a straight dislocation segment AB .

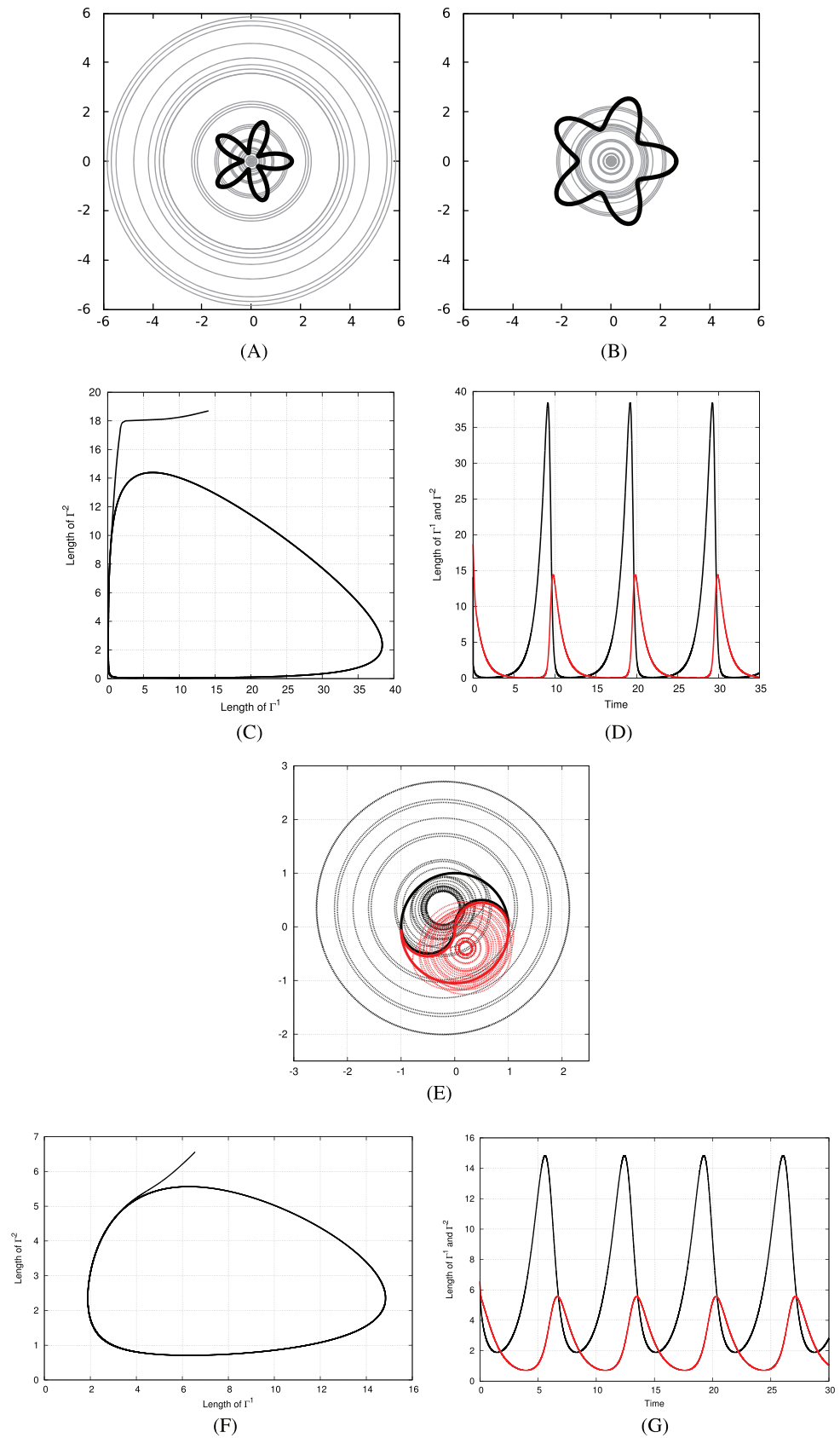


FIGURE 2 Periodically oscillating solutions of (19) for the initial 5-leaf shape and Ying-Yang shape curves Γ_{ini}^1 and Γ_{ini}^2 . A, B, and E, respectively. Phase portraits C, F and time evolution D, G of their total lengths [Colour figure can be viewed at wileyonlinelibrary.com]

Symbol	Meaning
\mathbf{T}	$\mathbf{T} = (T_1, T_2, T_3)^T$, $\mathbf{N} = \mathbf{T}^\perp$
\mathbf{R}	$\mathbf{R} = \mathbf{x} - \mathbf{A}$
R	$R = \ \mathbf{R}\ $
U	$U = \mathbf{R} \cdot \mathbf{T}$
\mathbf{Y}	$\mathbf{Y} = \mathbf{R} - RT$
\mathbf{Q}	The normal component of \mathbf{R}

TABLE 1 Table of symbols in the Devincre formula (5.2)

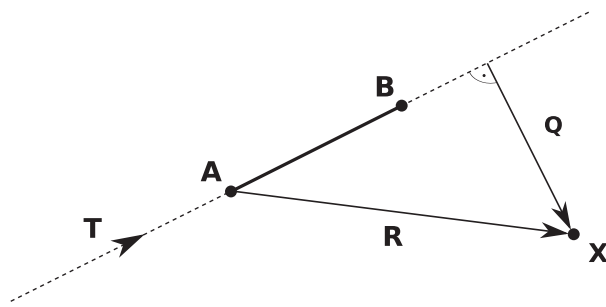


FIGURE 3 The stress field from a straight dislocation segment AB at a position \mathbf{x} . Vectors \mathbf{T} , \mathbf{Q} , and \mathbf{R} are related to the Devincre formula (5.2)

The Devincre formula³¹ provides a stress tensor $\sigma_{ij}^A(\mathbf{x})$ at a position \mathbf{x} from an infinite dislocation half-line going from the point A . It reads as follows:

$$\begin{aligned} \sigma_{ij}^A &= \frac{G}{4\pi R(U+R)} \left[(\mathbf{b} \times \mathbf{Y})_i T_j + (\mathbf{b} \times \mathbf{Y})_j T_i - \frac{1}{1-v} ((\mathbf{b} \times \mathbf{T})_i Y_j + (\mathbf{b} \times \mathbf{T})_j Y_i) \right. \\ &\quad \left. - \frac{\mathbf{b} \cdot (\mathbf{Q} \times \mathbf{T})}{1-v} \left[\delta_{ij} + T_i T_j + \frac{(Q_i T_j + Q_j T_i + U T_i T_j)(U+R)}{R^2} + \frac{Q_i Q_j (2+U/R)}{R(U+R)} \right] \right]. \end{aligned} \quad (21)$$

All symbols appearing in formula (5.2) are explained in Table 1 (see also Figure 3).

Then, the stress tensor at the position \mathbf{x} by a straight dislocation segment AB is given as the difference $\sigma_{ij}^{AB} = \sigma_{ij}^A - \sigma_{ij}^B$. The total stress σ_{ij}^1 exerted by a piece-wise linear dislocation curve Γ^2 is given as the sum over all linear segments of Γ^2 , i.e.

$$\sigma_{ij}^1(\mathbf{x}) = \sum_{AB \in \Gamma^2} \sigma_{ij}^{AB}.$$

In the continuous limit when $|AB| = ds^2 \rightarrow 0$ the above sum of stresses converges to the integral over the second curve Γ^2 , i.e.

$$\sigma_{ij}^1(\mathbf{x}) = \int_{\Gamma^2} \sigma_{ij}^{(2)}(\mathbf{X}(s^2)) ds^2,$$

where $\sigma_{ij}^{(2)}$ is the stress given by the infinitesimal segment of dislocation Γ^2 . To determine the interaction part of the force we apply the Peach-Koehler formula³²

$$\mathbf{F}_{int}^k = (\sigma_{ij}^k \mathbf{b}) \times \mathbf{T}^k. \quad (22)$$

In our model problem, we consider the Burgers vector $\mathbf{b} = (b, 0, 0)^T$ parallel to the x -axis and the slip planes parallel with the plane $y = 0$ in the xz coordinate system, and the unit tangential vector $\mathbf{T}^k = (T_1^k, 0, T_3^k)^T$ and the unit normal vector $\mathbf{N}^k = (T_3^k, 0, -T_1^k)^T$, $k = 1, 2$. Then, the acting force \mathbf{F}_{int}^k (22) can be expressed as follows:

$$\mathbf{F}_{int}^k = (\sigma_{ij}^k \mathbf{b}) \times \mathbf{T}^k = b(\sigma_{12}^k T_3^k, \sigma_{13}^k T_1^k - \sigma_{11}^k T_3^k, -\sigma_{12}^k T_1^k),$$

and its normal component is given by:

$$F_{int}^k = \mathbf{F}_{int}^k \cdot \mathbf{N}^k = b(\sigma_{12}^k (T_3^k)^2 + \sigma_{13}^k (T_1^k)^2) = b\sigma_{12}^k, \quad k = 1, 2.$$

As a consequence, for the resolved interaction stress, we have $\tau_{int}^k = \sigma_{12}^k$. Because we investigate interactions of dislocations in two parallel slip planes with a fixed distance $h_0 > 0$, it is clear that there is no singularity in the Devincre stress tensor (5.2) because

$$R \geq h_0 > 0, \quad \text{and } U + R = \mathbf{R} \cdot \mathbf{T} + \|\mathbf{R}\| \geq h_0 > 0.$$

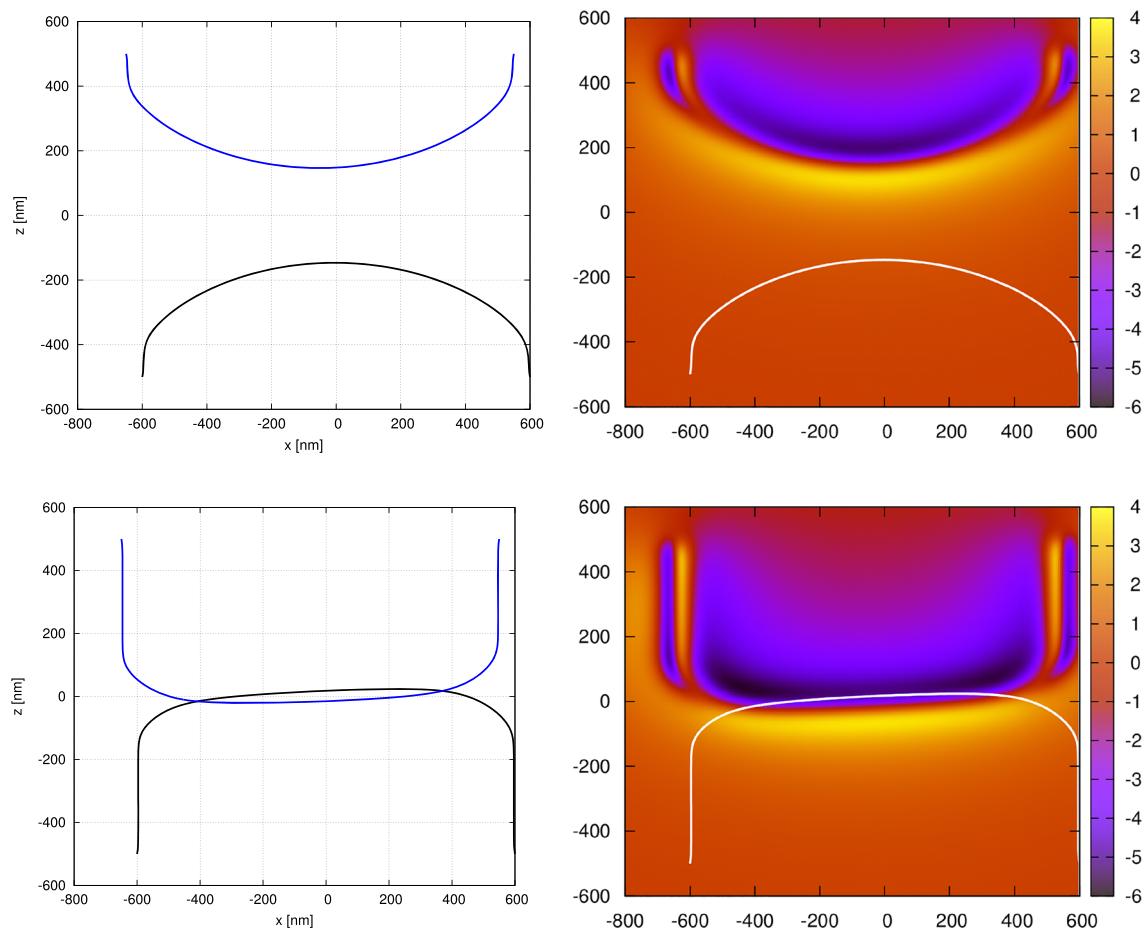


FIGURE 4 An example of two stages of a flow of two interacting dislocation loops in parallel slip planes (top-down view) under applied stress $\tau_{app} = 20$ MPa. In the left figures, both dislocation are drawn from top-down view. First, they evolve against each other and when they get sufficiently close, they became attracted by the mutual interaction forces and eventually remain in a dipole position. In the right figures, a single dislocation is depicted in white together with the color map of interaction stress (in megapascals) exerted by the second dislocation [Colour figure can be viewed at wileyonlinelibrary.com]

Now, if we project evolving curves into the plane $y = 0$, then their normal velocities can be written in the form of (1) with the external nonlocal source terms given by:

$$\mathcal{F}^1(\mathbf{x}^1, \Gamma^2) = \int_{\Gamma^2} f^1(\mathbf{x}^1, \mathbf{X}^2(s^2)) ds^2, \quad \mathcal{F}^2(\mathbf{x}^2, \Gamma^1) = \int_{\Gamma^1} f^2(\mathbf{X}^1(s^1), \mathbf{x}^2) ds^1,$$

where $f^k : \mathbb{R}^2 \times \mathbb{R}^2 \rightarrow \mathbb{R}$ are C^∞ smooth functions. Hence, we can apply Theorem 1 to obtain local existence, uniqueness, and continuation of classical Hölder smooth solutions. Furthermore, we can apply a numerical discretization scheme presented in section 4 in order to compute numerical solutions. An example of two stages of evolving dislocation loops is shown in Figure 4. Two initially straight dislocations bow in their persistent slip band (PSB) channels under applied stress $\tau_{app} = 20$ MPa. The loops evolve in parallel slip planes with the distance $h = 50$ nm. Dislocations and their respective channels are slightly off-centered, and eventually they reach the stable configuration and form the so-called dipole position. In the left figures, both dislocations are drawn from top-down view. In the right figures, a single dislocation is depicted in white together with the color map of interaction stress (in megapascals) exerted by the second dislocation.

6 | CONCLUSION

In this paper, we investigated a curvature driven geometric flow of several planar curves with mutual interactions that can have local as well as nonlocal character and the entire curve influences evolution of other curves. We proposed a direct Lagrangian approach for solving such a geometric flow of curves. We also proved local existence, uniqueness, and

continuation of Hölder smooth solutions to the governing system of nonlinear parabolic equations for the position vector parametrization of evolving curves. A numerical solution to the governing system has been constructed by means of the method of flowing finite volumes. Finally, we provided applications of the motion of interacting curves in nonlocal geometric flows of curves. We also demonstrated how the physical problem of motion of two interacting dislocation loops can be solved by means of the geometric flow of curves with nonlocal interactions.

ACKNOWLEDGEMENTS

This work does not have any conflicts of interest. M. Beneš was partly supported by the Ministry of Education, Youth and Sports of the Czech Republic under the Operational Programme Research, Development and Education (OP RDE) grant number CZ.02.1.01/0.0/0.0/16 019/0000778 “Centre for Advanced Applied Sciences,” group Material Science and Engineering. M. Kolář was supported by the International Research Fellowship of Japan Society for Promotion of Science. D. Ševčovič was supported by the Scientific Grant Agency (VEGA) grant 1/0062/18.

ORCID

Daniel Ševčovič  <https://orcid.org/0000-0002-1488-7736>

REFERENCES

1. Deckelnick K. Parametric mean curvature evolution with a Dirichlet boundary condition. *J Reine Angew Math.* 1995;459:37–60. <https://doi.org/10.1515/crll.1995.459.37>
2. Beneš M, Kimura M, Pauš P, Ševčovič D, Tsujikawa T, Yazaki S. Application of a curvature adjusted method in image segmentation. *Bull Inst Math Acad Sinica (N.S.)*. 2008;3:509–523.
3. Beneš M, Kratochvíl J, Kříšťan J, Minářík V, Pauš P. A parametric simulation method for discrete dislocation dynamics. *Eur Phys J Spec Top.* 2009;177:177–192. <https://doi.org/10.1140/epjst/e2009-01174-7>
4. Mikula K, Ševčovič D. Evolution of plane curves driven by a nonlinear function of curvature and anisotropy. *SIAM J Appl Math.* 2001;61:1473–1501. <https://doi.org/10.1137/S0036139999359288>
5. Mikula K, Ševčovič D. Computational and qualitative aspects of evolution of curves driven by curvature and external force. *Comput Vis Sci.* 2004;6:211–225. <https://doi.org/10.1007/s00791-004-0131-6>
6. Mikula K, Ševčovič D. A direct method for solving an anisotropic mean curvature flow of plane curves with an external force. *Math Methods Appl Sci.* 2004;27:1545–1565. <https://doi.org/10.1002/mma.514>
7. Pauš P, Beneš M, Kolář M, Kratochvíl J. Dynamics of dislocations described as evolving curves interacting with obstacles. *Model Simul Mater Sci.* 2016;24:035003. <https://doi.org/10.1088/0965-0393/24/3/035003>
8. Ševčovič D, Yazaki S. Evolution of plane curves with a curvature adjusted tangential velocity. *Japan J Ind Appl Math.* 2011;28:413–442. <https://doi.org/10.1007/s13160-011-0046-9>
9. Yazaki S. On the tangential velocity arising in a crystalline approximation of evolving plane curves. *Kybernetik.* 2007;43:913–918.
10. Pauš P, Kratochvíl J, Beneš M. A dislocation dynamics analysis of the critical cross-slip annihilation distance and the cyclic saturation stress in fcc single crystals at different temperatures. *Acta Mater.* 2013;61(20):7917–7923. <https://doi.org/10.1016/j.actamat.2013.09.032>
11. Ghoniem NM, Tong SH, Sun LZ. Parametric dislocation dynamics: a thermodynamics-based approach to investigations of mesoscopic plastic deformation. *Phys Rev B - Condensed Matter Materials Phys.* 2000;61(2):913–927. <https://doi.org/10.1103/PhysRevB.61.913>
12. Visintin A. *Models of Phase Transitions*. Boston: Birkhäuser; 1996.
13. Kobayashi R. Modeling and numerical simulations of dendritic crystal growth. *Physica D.* 1993;63:410–423. [https://doi.org/10.1016/0167-2789\(93\)90120-P](https://doi.org/10.1016/0167-2789(93)90120-P)
14. Schmidt A. Computation of three dimensional dendrites with finite elements. *J Comput Phys.* 1996;125:293–312. <https://doi.org/10.1006/jcph.1996.0095>
15. Beneš M. Mathematical analysis of phase-field equations with numerically efficient coupling terms. *Interfaces Free Bd.* 2001;3:201–221. <https://doi.org/10.4171/IFB/38>
16. Hallberg H. Approaches to modeling of recrystallization. *Metals.* 2011;1:16–48. <https://doi.org/10.3390/met1010016>
17. Epstein CL, Gage M. The curve shortening flow. In: Chorin AJ, Majda AJ (eds) *Wave Motion: Theory, Modelling, and Computation. Mathematical Sciences Research Institute Publications*, vol 7, Springer, New York; 1987. DOI: https://doi.org/10.1007/978-1-4613-9583-6_2.
18. Kolář M, Beneš M, Ševčovič D. Computational analysis of the conserved curvature driven flow for open curves in the plane. *Math Comput Simulation.* 2016;126:1–13. <https://doi.org/10.1016/j.matcom.2016.02.004>
19. Hou TY, Lowengrub J, Shelley M. Removing the stiffness from interfacial flows and surface tension. *J Comput Phys.* 1994;114:312–338. <https://doi.org/10.1006/jcph.1994.1170>
20. Kimura M. Numerical analysis for moving boundary problems using the boundary tracking method. *Japan J Indust Appl Math.* 1997;14:373–398. <https://doi.org/10.1007/BF03167390>
21. Angenent S. Nonlinear analytic semiflows. *Proc R Soc Edinb, Sect A.* 1990;115:91–107. <https://doi.org/10.1017/S0308210500024598>

22. Angenent S. Parabolic equations for curves on surfaces. I: curves with p -integrable curvature. *Annal Math.* 1990;132(2):451–483. <https://doi.org/10.2307/1971426>
23. Lunardi A. Abstract quasilinear parabolic equations. *Math Ann.* 1984;267:395–416. <https://doi.org/10.1007/BF01456097>
24. Gage M. On an area-preserving evolution equation for plane curves. *Contemp Math.* 1986;51:51–62.
25. Hirsch PB, Horne RW, Whelan MJ. Direct observations of the arrangement and motion of dislocations in aluminium. *Philos Mag J Theor Exp Appl Phys.* 1956;1:677–684. <https://doi.org/10.1080/14786430600844674>
26. Bulatov VV, Cai W. *Computer Simulations of Dislocations*. Oxford University Press; 2006.
27. Markov IV. *Crystal Growth for Beginners: Fundamentals of Nucleation, Crystal Growth, and Epitaxy*. 2nd ed. World Scientific Publishing Company; 2004.
28. Mura M. *Micromechanics of Defects in Solids*. Netherlands: Kluwer Academic Publishers Group; 1987.
29. Hull D, Bacon D. *Introduction to Dislocations*. Butterworth-Heinemann; 2001.
30. Kolář M, Beneš M, Ševčovič D. Mathematical model and computational studies of discrete dislocation dynamics. *IAENG Int J Appl Math.* 2015;45(3):198–207.
31. Devincre B. Three dimensional stress field expression for straight dislocation segment. *Solid State Commun.* 1995;93(11):875–878. [https://doi.org/10.1016/0038-1098\(94\)00894-9](https://doi.org/10.1016/0038-1098(94)00894-9)
32. Peach M, Koehler JS. The forces exerted on dislocations and the stress fields produced by them. *Phys Ther Rev.* 1950;80:436–439. <https://doi.org/10.1103/PhysRev.80.436>

How to cite this article: Beneš M, Kolář M, Ševčovič D. Curvature driven flow of a family of interacting curves with applications. *Math Meth Appl Sci.* 2020;43:4177–4190. <https://doi.org/10.1002/mma.6182>